3 Modelling coal devolatilization behaviour

3.1 Introduction

A description of the complex mixture of de-polymerisation, cross-linking, hydrogen transfer, substitution and re-polymerisation reactions occurring during coal devolatilization presents a challenging task from a modelling perspective. The development and implementation of a suitable model to predict coal devolatilization behaviour, as a function of operating parameters such as temperature, heating rate and particle size provide a valuable tool for simulating typical coal conversion reactors. In particular, devolatilization modelling of powdered and small particles are restricted to typical chemical reaction controlled conditions and have received overwhelming attention in the past few decades. Differences observed in the behaviour of large coal particles have therefore led researchers to employ a more rigorous treatment of comprehensive devolatilization models. In addition, an understanding of the behaviour of coal particles involved in lump coal conversion processes necessitates the combination of typical reaction kinetics as well as heat- and mass transport effects and has only recently received increasing attention. The development of such a particle model facilitates the initial step in understanding the overall behaviour of lump coal conversion and should be based on both fundamental principles, as well as the success at which it has been applied in previous work in literature.

A detailed account of the choice, description and evaluation of the model will be provided in this chapter. Sub-models for intrinsic kinetics, heat- and mass transport are discussed separately in the text. An overview of the choice of kinetic model used is provided in Section 3.2, while the evaluation procedure is elaborated on in Section 3.3. Furthermore, the importance and description of transport phenomena as well as the evaluation procedure of the overall model describing the devolatilization of large coal particles is attended to in Sections 3.4 and 3.5, respectively, whereafter some conclusive remarks will be given in Section 3.6.

3.2 Choice and description of an appropriate kinetic model

Systematic research during the past few decades has advanced our knowledge of the kinetics and mechanisms of the devolatilization process and provided valuable techniques for predicting, to a reasonable extent, the behaviour of coals (Smoot & Pratt, 1979; Smoot, 1981; Yue, 1995). Devolatilization modelling is, however, quite straightforward if the chemical reaction is rate controlling and the fuels under investigation are of a simple characteristic nature. Kinetic models range in different levels of complexity from free radical mechanistic models for simple hydrocarbons such as propane (Trimm & Turner, 1981) to more complex reaction schemes involving numerous amounts of individual reactions, incorporating extra transport steps such as in the case for naphtha devolatilization (Kumar & Kunzru, 1985). The kinetic description of more complex poly-aromatic substances such as coal therefore presents a difficult task, due to a vast amount of reactions involved. The devolatilization of coal is normally studied at the hand of pseudo-mechanistic models (Conesa et al., 2001), which entails that the overall measured reaction rate is the cumulative effect of numerous separate reactions (Lázaro et al., 1998). For coal devolatilization a large number of possible modelling strategies are available of which the simplest are empirical in nature and employ global kinetics (Arenillas et al., 2001; Conesa et al., 2001; Lu & Do, 1991; Lázaro et al., 1998). The change of rate with temperature is generally described by the Arrhenius expression. In addition, these models are further subdivided into single- and multiple reaction schemes such as the DAEM. A detailed account of these models is provided in Section 2.6. Current advances in the evaluation of the physiochemical properties of the coal structure has also led to the development of more advanced network models such as the FG-DVC (Solomon *et al.*, 1993) and FLASHCHAIN (Niksa & Kerstein, 1991) model.

The choice of a suitable kinetic model should therefore bear relevance to the process under investigation. For this investigation the devolatilization behaviour of coal entails the evaluation of the total mass loss behaviour of the amount of volatile matter and not of individual species. The mass loss behaviour will therefore be described at the hand of global kinetics involving the description of one or more lumped components as outlined in typical series or parallel first-order reaction schemes or the more advanced DAEM. The aim of this modelling exercise is therefore to propose a global intrinsic kinetic model that can be included into a large particle model, which allows for the description of transport phenomena during large coal particle devolatilization.

3.3 Model description and evaluation of intrinsic kinetics

3.3.1 Kinetic model description

3.3.1.1 Determination of the kinetic parameters

Global devolatilization kinetics for the description of overall weight losses have been used extensively by numerous authors including Alonso *et al*. (2001), Gürüz *et al*. (2004), Lázaro *et al*. (1998) and Yip *et al*. (2009). The most commonly used intrinsic kinetic model for assessing global kinetics is based on a unimolecular n^{th} order single reaction rate model as defined mathematically in Equation 3.1 (Burnham & Braun, 1999; Donskoi & McElwain, 1999).:

$$\frac{dX}{dt} = k \cdot (1 - X)^n \qquad \text{Equation (3.1)}$$

where X represents the fractional conversion of volatiles released at time t and k is defined as the overall reaction rate constant of which the temperature dependence is described by the Arrhenius equation (Eq.(3.2)):

$$k = k_0 \cdot \exp\left(\frac{-E_a}{RT}\right) \qquad \text{Equation (3.2)}$$

The reaction order (n) of the reaction equation presented in Equation (3.1) is either assumed to be first- or second-order (Bliek *et al*., 1985; Kök *et al*., 1998; Kristiansen, 1996; Strezov *et al*., 2004; Yip *et al*., 2009) or estimated through regression of the experimental data (Alonso *et al*., 2001; Gürüz *et al*., 2004). Derivation of the kinetic triplets (k_0, E_a and n) requires knowledge of the time- or temperature history of mass loss during devolatilization. The norm, however, for kinetic studies is to conduct reactions under isothermal conditions, especially for fast reactions such as devolatilization at high temperatures. Time-resolved measurements of coal devolatilization are therefore very difficult and present uncertainty due to the fact that the devolatilization process normally completes within a few seconds before the isothermal state is reached (Lázaro *et al*., 1998). Currently non-isothermal techniques have proven to be more useful than isothermal techniques for deriving the kinetic triplets (Alonso *et al*., 2001; Lázaro *et*

al., 1998). If constant, linear heating rate ($T = T_i + \beta t$) measurements are employed Equation (3.1) can be rewritten as (Yongjiang *et al*., 2011):

$$\int_0^X \frac{dX}{(1-X)^n} = \frac{k_0}{\beta}\int_{T_0}^{T} \exp\left(\frac{-E_a}{RT}\right)\cdot dT \qquad \text{Equation (3.3)}$$

The right hand side of Equation (3.3) is generally referred to as the temperature integral and has no exact analytical solution (Aboulkas *et al*., 2011; Alonso *et al*., 2001; Yue, 1995). A large amount of numerical approximations are however available to evaluate the non-isothermal model equation as presented in Equation (3.3). A summary of the important numerical methods used for a first-order reaction rate model is provided in Table 3.1.

Table 3.1 Summary of methods for determining the kinetic parameters of the first-order model.

Analysis method	*Mathematical equation*	*Equation no.*
Direct Arrhenius plot method (Yongjiang *et al*., 2011)	$\ln\left(\frac{1}{1-X}\cdot\frac{dX}{dT}\right) = \ln\left(\frac{k_0}{\beta}\right) - \frac{E_a}{RT}$	Equation (3.4)
Integral method (Shih & Sohn, 1980)	$-\ln(1-X) = \frac{k_0}{\beta}\left[Te^{-E_a/RT} + \frac{E_a}{R}\cdot E_1\cdot\left(-\frac{E_a}{RT}\right)\right]$	Equation (3.5)
Friedman method (Friedman, 1964)	$\ln\left(\beta\frac{dX}{dT}\right) - \ln(1-X) = \ln(k_0) - \frac{E_a}{RT}$	Equation (3.6)
Coats-Redfern method (Coats & Redfern, 1964)	$\ln\left(\frac{-\beta\ln(1-X)}{RT^2}\right) = \ln\left(\frac{k_0}{E_a}\right)\cdot\left[1-\frac{2RT}{E_a}\right] - \frac{E_a}{RT}$	Equation (3.7)
Chen-Nuttall method (Thakur & Nuttall, 1987)	$\ln\left(\frac{-\beta\cdot(E_a+2RT)}{RT^2}\cdot\ln(1-X)\right) = \ln(k_0) - \frac{E_a}{RT}$	Equation (3.8)
Explicit one-step method (Alonso *et al*., 2001)	$X_i = 1-\exp\left[\ln(1-X_{i-1}) - \int_{t_{i-1}}^{t_i} k_0\exp\left(\frac{-E_a}{RT}\right)dt\right]$	Equation (3.9)
Anthony-Howard model (Howard *et al*., 1976)	$X = 1-\int_0^\infty \exp\left[-\int_0^t k_0\exp\left(\frac{-E_a}{RT}\right)dt\right]\cdot f(E_a)dE$	Equation (3.10a)
	in which: $f(E_a) = \left(\frac{1}{\sigma\sqrt{2\pi}}\right)\exp\left[\frac{-(E_a-E_0)^2}{2\sigma^2}\right]$	Equation (3.10b)

Details regarding the derivation procedures of the different models can be found in literature (Yue, 1995; Yongjiang *et al*., 2011). The use of more direct integral approaches (not shown in the above table) has also been reported (Aboyade *et al*., 2012; Caballero & Conesa, 2005). A comparison between the above methods revealed that some accuracy constraints occur, but that the integral method is normally the most recommended strategy (Yue, 1995; Yongjiang *et al*., 2011). Of all the methods currently proposed, the DAEM (Anthony-Howard model) has been shown to be the most powerful model for predicting devolatilization behaviour (Arenillas *et al*., 2001; Braun & Burnham, 1987; Cai & Liu, 2008; Donskoi & McElwain, 1999 & 2000; Heidenreich *et al*., 1999; Mani *et al*., 2009). For the case of the DAEM, the distribution in reactivity caused by the reaction complexity is attributed to the occurrence of a set of *m* independent, first-order, parallel reactions with their own characteristic values of k_0 and E_a (Alonso *et al*., 2001). A simplistic approach for solving the DAEM considers a common, constant frequency factor applicable for all activation energies in the distribution (Burnham *et al.,* 1995). This simplification has, however, been criticised by Alonso *et al*. (2001) who believes that the isokinetic effect, which involves the relationship between frequency factor and activation energy, cannot be neglected in the calculation procedure. This was also the general approach adopted by Mianowski and Radko (1993); and Misra and Essenhigh (1988). The use of continuous distribution curves (*i.e*., Gaussian), for the description of overall activation energy by a constant average activation energy and a standard deviation of energies (σ) has also raised concerns (Mianowski & Radko; 1993; Miura, 1995).

3.3.1.2 Compensation effect of kinetic parameters

Variations in the kinetic parameters determined by a single overall reaction model from non-isothermal thermogravimetric curves have been extensively encountered in literature (Constable, 1925; Narayan & Antal, 1996; Olivella & de las Heras, 2006; Olivella & de las Heras, 2008; Yue, 1995). These variations are encountered due to physico-chemical properties, measuring conditions and the mathematical strategies employed to determine the parameters. A subsequent increase or decrease in the kinetic parameters with increasing heating rate has been observed by authors such as Olivella and de las Heras (2008) and Yue (1995). Accordingly, in order to ascertain the same rate constant at different conditions, high values of activation energy would be compensated by high values of the frequency factor. This mutual dependence is normally referred to as the kinetic compensation effect and can be expressed by the following equation (Yue, 1995):

$$\ln k_0 = \alpha E_a + \delta$$ Equation (3.11)

When the above equation is reproduced on Arrhenius coordinates with an intersection point through the isokinetic points ($1/T_{iso}$ and lnk_{iso}) then the relationship can be given as (Yue, 1995):

$$\ln k = a + b \cdot \frac{1}{T}$$ Equation (3.12)

It should be noted that Equation (3.12) is a special case derived from Equation (3.11) and the existence thereof guarantees the existence of the compensation effect. In contrast, the existence of Equation (3.11) does not guarantee the existence of the isokinetic relationship (Yue, 1995). Details regarding the factors attributing to the existence of the compensation and isokinetic effect can be found elsewhere (Yue, 1995).

3.3.2 Kinetic model evaluation

The use of powdered coal samples in non-isothermal work is normally recommended in order to ensure that the effects of heat- and mass transfer are limited during the determination of the intrinsic kinetic parameters (Aboyade *et al*., 2012; Antal & Várhegyi, 1995; Yang *et al*., 2007). In addition, the process of de-convolution of DTG curves of model- and less complex carbon-containing compounds (such as biomass and oil shales) into pseudo-component curves have been found to be much easier when compared to de-convolution of DTG curves obtained for coals (Aboulkas et *al*., 2011; Aboyade *et al*., 2011; Grønli *et al*., 2002). This challenge necessitates the need for further elaboration on the behaviour of typical DTG curves of coals, in order to formulate and evaluate an appropriate model. A typical hypothetical DTG curve (for illustration purposes) of the devolatilization behaviour of coal is provided in Figure 3.1 and corresponds to what was obtained in previous investigations (Aboyade *et al*., 2012; Alonso *et al*., 1999 & 2001). As illustrated in Figure 3.1, the DTG curve is characterised by a peak (peak (a)) in the low temperature region with a maximum rate occurring between 40℃ and 100℃ and corresponds to the initial release of absorbed moisture. In some cases an adjacent peak to the absorbed moisture peak is observed, annotated as peak (b), which has been attributed to either the release of crystal water associated with inherent minerals or chemically bonded moisture (Alonso *et al*., 2001; Boiko, 2000).

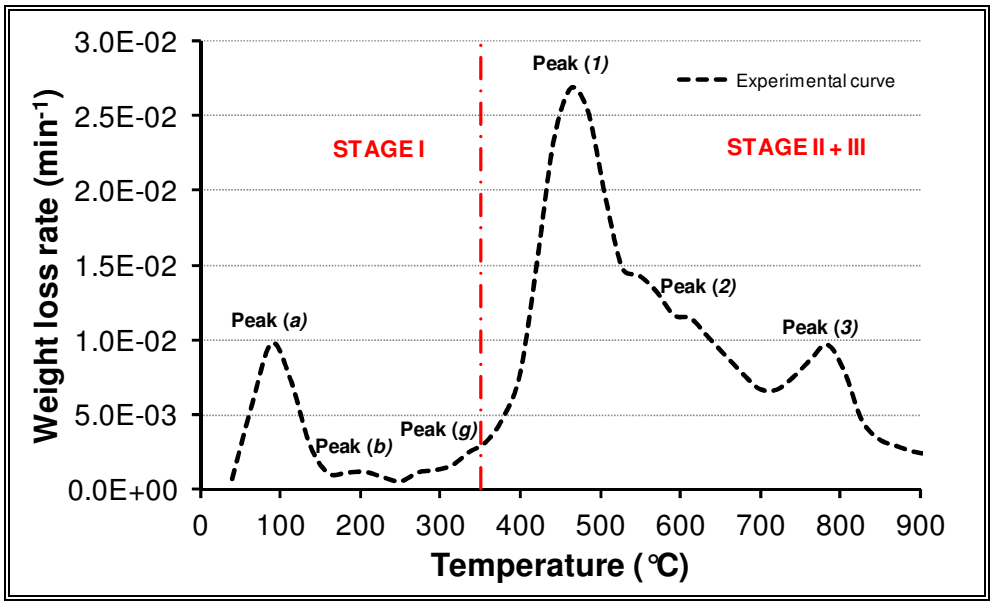

Figure 3.1 Hypothetical DTG curve of coal devolatilization (adapted from Alonso *et al.* (2001)).

In addition, the simultaneous vaporization and transport of so-called "guest" molecules (molecular phase) as described by peak (g) start to occur (Solomon *et al.*, 1992). The presence of peak (g) corresponds to stage I of the model proposed by Serio *et al.* (1987) and is not considered to be part of the primary devolatilization process. The occurrence of peaks (a), (b) and (g) is therefore eliminated in some works prior to the investigation of the main devolatilization zone (stage II & III) (Alonso *et al.*, 2001). For large particle applications, this is, however, not the case as the drying zone forms an integral part of the process (Bunt & Waanders, 2008). In addition, the presence of inherent moisture as steam from an operating perspective can increase the volume of evolved gases, cool down the reacting medium, decrease the gas mixture temperature and subsequently decrease the devolatilization rate (Bellais, 2007). The evaporation of moisture from porous media involves complicated heat- and mass transfer mechanisms and the availability of a comprehensive model is limited (Yip *et al.*, 2009). Detail mechanistic schemes for wood drying and -devolatilization have been proposed by authors such as Bellais (2007) and Grønli (1996). The formulation of an appropriate mathematical model describing the evaporation rate of moisture is a tedious task and models such as the heat sink model, first-order evaporation rate model and the equilibrium model have generally been used (Bellais, 2007). The work of Bellais (2007) has shown that no significant difference could be observed in the type of model used for describing moisture evaporation from wood particles. In a number of investigations, the evaporation of moisture from the coal matrix is described by an additional first-order reaction expression, due to its integratability into the

overall kinetic scheme and the conservation laws (Abhari & Isaacs, 1990; Bellais, 2007; Li *et al*., 2009; Yip *et al.,* 2009). The first-order expression for moisture evolution will therefore be used in this investigation.

The main devolatilization zone (stage II & III) constitutes the release of tar (II), primary gases (II), secondary gases (III) and the subsequent formation of char (Alonso *et al.,* 2001; Serio *et al*., 1987). The evolution profile of stage II and III comprises two quite distinguishable peaks (peaks (1) and (3)) and a less observable peak (peak (2)) and is in agreement with what was observed for coal devolatilization by van Heek and Hodek (1994). The extensive asymmetric nature of the DTG curve of coal devolatilization therefore makes the use of a single first-order reaction model impractical in determination of the kinetic parameters. In a response to this, authors such as Alonso *et al*. (2001) formulated a lumped first-order model allowing for the fraction contribution (ξ) made by the different individual peaks. Accordingly the following reaction rate equation can be used for the entire temperature range under investigation:

$$\frac{dX}{dt} = \xi_a \frac{dX_a}{dt} + \xi_b \frac{dX_b}{dt} + \xi_g \frac{dX_g}{dt} + \sum_{i=1}^{3} \xi_i \frac{dX_i}{dt} \qquad \text{Equation (3.13)}$$

If stages I, II and III are lumped together and the ultimate amount of volatiles and moisture (V^*_t) is included, then Equation (3.13) can be rewritten as:

$$\frac{dV_t}{dt} = V_t^* \cdot \sum_{i=j}^{j} \xi_i k_{i,0} \cdot \exp\left(\frac{-E_{a,i}}{RT}\right) \cdot (1 - X_i); \quad j = a, b, g, 1, 2, 3 \qquad \text{Equation (3.14a)}$$

The intrinsic reaction rates for moisture evaporation and volatile evolution can therefore be described as:

$$R_v = \rho_{s,0} \cdot V_{t,v}^* \frac{dX_v}{dt} \text{ and } R_a = \rho_{s,0} \cdot V_a^* \frac{dX_a}{dt} \qquad \text{Equation (3.14b)}$$

The intrinsic parameters describing the different stages of the devolatilization process can be estimated by numerical integration of the above equation by the methods proposed in Section 3.3.1.1. This can be accomplished with the aid of a typical numerical mathematical package

such as MATLAB® or FORTRAN®. The determination of a single set of kinetic parameters and the fractions of contribution describing the overall reaction rate of each pseudo-component at different heating rates involves the use of multi-dimensional non-linear regression that minimizes the objective function (*OBF*) over all heating rates. This method was successfully applied by Aboyade *et al*. (2012) on the devolatilization behaviour of blends of coal and biomass. The objective function used is provided in Equation (3.15):

$$OBF = \sum_{k=1}^{N_k} \sum_{m=1}^{N_m} \left[\left(\frac{dX}{dt} \right)_{\exp} - \left(\frac{dX}{dt} \right)_{calc} \right]^2 \qquad \text{Equation (3.15)}$$

In addition Equation (3.16) can be used to test the validity of the predicted model values on the quality of fit (*QOF*) of the experimental data (for each heating rate as well as overall process).

$$QOF\ (\%) = 100 \times \sum_{m=1}^{N_m} \frac{\sqrt{\left[\left(dX/dt \right)_{\exp} - \left(dX/dt \right)_{calc} \right]^2 / N_m}}{\max \left| dX/dt \right|_{\exp}} \qquad \text{Equation (3.16)}$$

N_k in Equation (3.16) can be replaced by the product of N_k and N_m in order to estimate a global *QOF* valid over all heating rates (Aboyade *et al.,* 2012).

3.4 Inclusion of physical transport effects

The development of an overall model for simulating devolatilization behaviour of large coal particles necessitates the need for the inclusion of heat- and mass transfer effects. Large particle devolatilization can therefore be described by three main processes (as shown in Figure 3.2), which involve: (1) heat transfer to (convective and radiative transfer), from (radiative transfer) and inside the coal particle (conductive heat transfer and heat losses due to reaction, evaporation and product transport in coal/char pores), (2) kinetics of volatile evolution and moisture release; and (3) intraparticle mass transfer of volatile species (Agarwal *et al*., 1984a & b; Stubington & Sumaryono, 1984; Tomeczek & Kowol, 1990). Numerous investigations on the determination of a comprehensive mathematical model for describing large particle devolatilization have led to the general conclusion that heat transfer and chemical kinetics are rate controlling for the overall mechanism (Agarwal *et al*., 1984a & b; Heidenreich *et al*., 1999;

Stubington & Sumaryono, 1984; Tomeczek & Kowol, 1990; Wildegger-Gaissmaier & Agarwal, 1990).

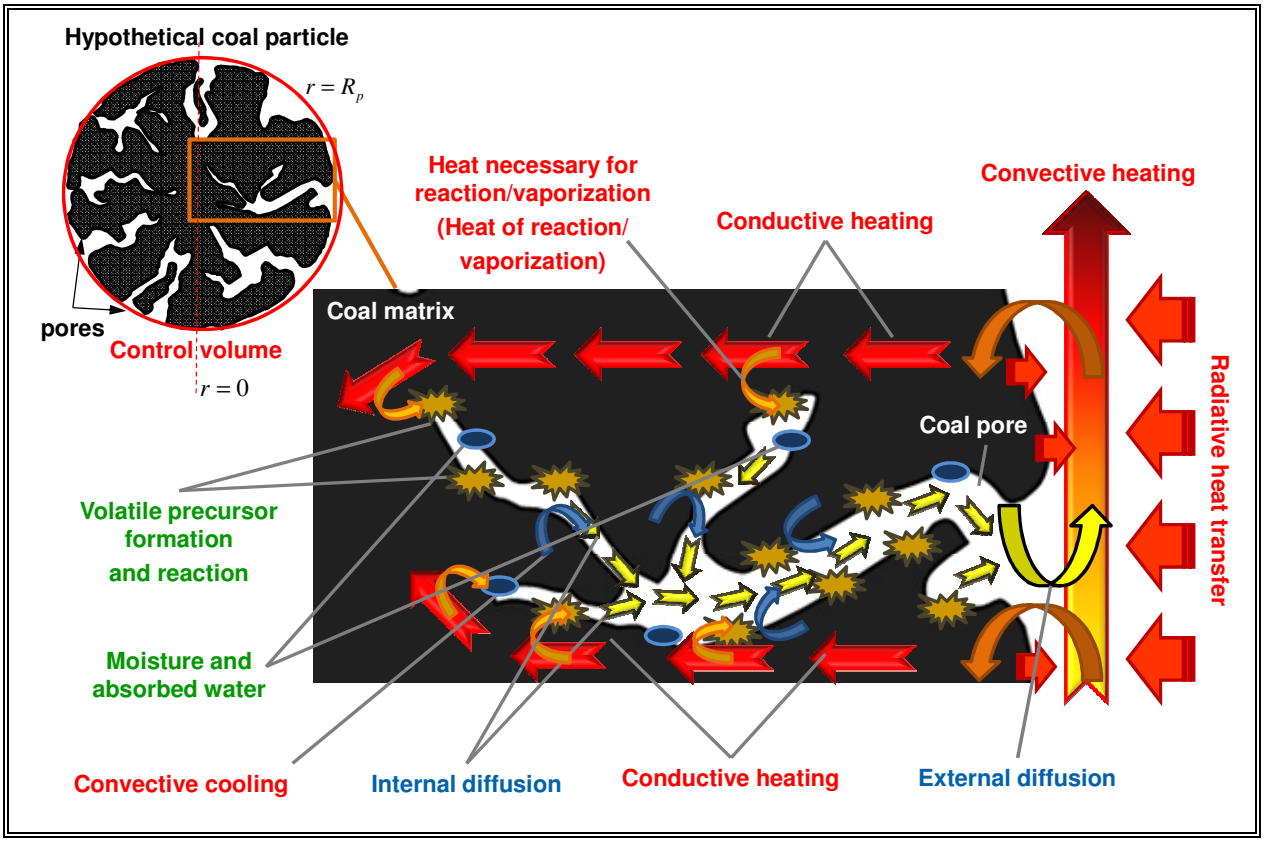

Figure 3.2 Transport and reaction processes during large particle coal devolatilization.

From a mass transfer perspective, Koch *et al*. (1969) suggested that the char layer forming around the devolatilizing particle provides negligible resistance to the transport of volatiles from the particle. In addition, for low rank coals Anthony *et al*. (1975) indicated that the effect of pressure on lignite devolatilization was negligible. This concept was challenged by authors who provided evidence that the role of mass transfer cannot be neglected due to internal convection of volatiles (Bliek *et al*., 1985; Tsang, 1980), secondary deposition reactions (Bliek *et al*., 1985) and coal particle swelling (Sadhukhan *et al*., 2011). A model accounting for all the preceding concepts and one of the most comprehensive models thus far was proposed by Sadhukhan *et al*. (2011). Application of this model, with the addition of additional descriptive equations to the current investigation, will form the basis for the model describing transport effects. The descriptive partial differential- and auxiliary equations used for heat- and mass transfer will be discussed separately.

3.4.1 Heat transfer considerations

The coal energy equation is based on the unsteady state, infinitesimal, control volume heat equation for a single, solid spherical particle (Sadhukhan *et al.*, 2011). The equation is formulated in Equation (3.17a) with the assumption that volatile matter and solid coal are in thermal equilibrium; and that the coal particle volume remains relatively constant (no swelling and/or shrinkage) throughout the devolatilization process:

$$c_{p,s}\frac{\partial(\rho_s T_s)}{\partial t}=\frac{1}{r^2}\left[k_s\cdot\left(\frac{\partial}{\partial r}r^2\frac{\partial T_s}{\partial r}\right)-\sum_{i=a,v}c_{p,i}\cdot\frac{\partial}{\partial r}\left(r^2 u\rho_i T_s\right)\right]+R_v\left(-\Delta H_r\right)+R_a\left(-\Delta H_{vap,a}\right)$$

Equation (3.17a)

Incorporation of the effect of volume change due to particle swelling/shrinkage requires the multiplication of both sides of Equation (3.17a) with the particle volume as shown in Equation (3.17b):

$$vc_{p,s}\frac{\partial(\rho_s T_s)}{\partial t}=\frac{v}{r^2}\left[k_s\cdot\left(\frac{\partial}{\partial r}r^2\frac{\partial T_s}{\partial r}\right)-\sum_{i=a,v}c_{p,i}\cdot\frac{\partial}{\partial r}\left(r^2 u\rho_i T_s\right)\right]+vR_v\left(-\Delta H_r\right)+vR_a\left(-\Delta H_{vap,a}\right)$$

Equation (3.17b)

Assuming the change in particle volume to be time dependent leads to the following expression for the general heat equation:

$$c_{p,s}\frac{\partial(v\rho_s T_s)}{\partial t}=\frac{v}{r^2}\left[k_s\cdot\left(\frac{\partial}{\partial r}r^2\frac{\partial T_s}{\partial r}\right)-\sum_{i=a,v}c_{p,i}\cdot\frac{\partial}{\partial r}\left(r^2 u\rho_i T_s\right)\right]+vR_v\left(-\Delta H_r\right)+vR_a\left(-\Delta H_{vap,a}\right)$$

Equation (3.17c)

Application of the chain rule to the differential term on the left hand side provides an expression that accounts for any heat losses due to particle swelling and/or shrinkage:

$$vc_{p,s}\frac{\partial(\rho_s T_s)}{\partial t}+c_{p,s}\rho_s T_s\frac{\partial v}{\partial t}=\frac{v}{r^2}\left[k_s\cdot\left(\frac{\partial}{\partial r}r^2\frac{\partial T_s}{\partial r}\right)-\sum_{i=a,v}c_{p,i}\cdot\frac{\partial}{\partial r}\left(r^2 u\rho_i T_s\right)\right]+vR_v\left(-\Delta H_r\right)+vR_a\left(-\Delta H_{vap,a}\right)$$

Equation (3.17d)

Rearranging terms and division by the volume term (v) yields the following equation as proposed by Sadhukhan *et al.*, (2011):

$$c_{p,s}\frac{\partial(\rho_s T_s)}{\partial t}=\frac{1}{r^2}\left[k_s\cdot\left(\frac{\partial}{\partial r}r^2\frac{\partial T_s}{\partial r}\right)-\sum_{i=a,v}c_{p,i}\cdot\frac{\partial}{\partial r}\left(r^2 u\rho_i T_s\right)\right]+R_v\left(-\Delta H_r\right)+R_a\left(-\Delta H_{vap,a}\right)-\frac{c_{p,s}\rho_s T_s}{v}\frac{\partial v}{\partial t}$$

Equation (3.17e)

With the boundary and initial conditions defined as (Sadhukhan *et al.*, 2011):

At $t=0$ for $0\le r\le R_p$; $\quad T_s=T_i$ Equation (3.18a)

For $t>0$ at $r=0$; $\quad -k_s\frac{\partial T_s}{\partial r}+u\rho_v c_{p,v}T_s+u\rho_a c_{p,a}T_s=0$ Equation (3.18b)

For $t>0$ at $r=R_p$; $\quad -k_s\frac{\partial T_s}{\partial r}+u\rho_v c_{p,v}T_s+u\rho_a c_{p,a}T_s=\sigma_b\varepsilon_{rad}\left(T_s^4-T_f^4\right)+h_{conv}\left(T_s-T_f\right)$

Equation (3.18c)

A comparison with particle heat equations used by other authors reveals the inclusion of a convective cooling term for heat removed by both moisture and volatiles moving through the porous matrix (2nd summed term on the right of Equation (3.17e)), heat loss due to reaction (3rd term on the right of Equation (3.17e)), heat loss due to the vaporization of water (4th term on the right of Equation (3.17e)) and heat change due to particle swelling/shrinkage (5th term on the right of Equation (3.17e)). The solution of Equation (3.17e) requires an extensive knowledge of the characteristic parameters defining both the solid phase as well as the gaseous (volatile) phase. Characteristic parameters for the solid phase (coal particle) include: particle density (ρ_s), specific heat ($c_{p,s}$), effective thermal conductivity (k_s), enthalpy of reaction (ΔH_r), particle volume (v) and emissivity (ε_{rad}), while heat capacity ($c_{p,v}$), and volatile density (ρ_v) form the important characteristic parameters for the volatile phase. Characteristic properties for inherent moisture are similar to those needed for the physical description of volatiles. A major limitation from other investigations is the choice of heat transfer parameters to solve the generic heat equation. Some investigations assume constant thermophysical properties for the coal itself in order to simplify the numerical solution of the above equation (Agarwal, 1985; Agarwal *et al.*, 1987). A combination of physical constants and empirical auxiliary models can be utilized for a description of the thermophysical properties as a function of the operating conditions. Due to the

complexity of the devolatilization process, either assumed constants or empirical correlations are employed for determining the physical properties of coal, inherent moisture and especially volatile matter. The empirical correlations and/or -models for determining the thermophysical properties needed to solve Equation (3.17e) are summarised in Table 3.2.

Table 3.2 Summary of important correlations for thermophysical properties.

Thermophysical property	***Empirical correlation/equation***	***Equation no.:***
Solid effective heat conductivity (Badzioch & Hawksley, 1970; Heidenreich *et al.*, 1999)	$k_s = 0.19; \quad T_s \le 573\,K$ or $k_s = 0.23; \quad T_s \le 673\,K$ $k_s = 0.19 + 2.5\times10^{-4}\cdot(T_s - 573)$; $T_s > 573\,K$ or $k_s = 0.23 + 2.24\times10^{-5}\cdot(T_s - 673)^{1.8}$; $T_s > 673\,K$ Unit: [W.m^{-1}.K^{-1}]	Equation (3.19) Equation (3.20)
Volumetric specific heat capacity (Badzioch & Hawksley, 1970)	$\rho_s c_{p,s} = 1.92\times10^{6}; \quad T_s \le 623\,K$ $\rho_s c_{p,s} = 1.92\times10^{6} - 2.92\times10^{3}\cdot(T_s - 623); \quad T_s > 623\,K$ Unit: [J.m^{-3}.K^{-1}]	Equation (3.21)
Specific heat of water vapour (Grønli, 1996)	$c_{p,a} = 1670 + 6.4\times10^{-1}T_s$ Unit: [J.kg^{-1}.K^{-1}]	Equation (3.22)
Heat capacity of volatiles (Bharadwaj *et al.*, 2004)	$c_{p,v} = -100 + 4.4T_s - 1.57\times10^{-3}T_s^{2}$ Unit: [J.kg^{-1}.K^{-1}]	Equation (3.23)
External heat transfer coefficient (Kunii & Levenspiel, 1969)	$h_{conv} = \frac{k_g}{d_p}\left(2 + 0.6\cdot \mathrm{Re}^{0.5}\cdot \mathrm{Pr}^{0.333}\right)$ Unit: [W.m^{-2}.K^{-1}]	Equation (3.24)
Effective emissivity (Incropera *et al.*, 2007)	$\varepsilon_{rad} = \frac{1}{\frac{1}{\varepsilon_{rad,s}} + \frac{1-\varepsilon_{rad,t}}{\varepsilon_{rad,t}}\cdot\left(\frac{r_p}{r_t}\right)}$ Unit: [-]	Equation (3.25)
Heat of evaporation (Bellais, 2007)	$\Delta H_{vap,a} = 3179\times10^{3} - 2500T_s$ Unit: [J.kg^{-1}]	Equation (3.26)

Values of constants used in the heat equation are provided in Table 3.3. A number of investigations have revealed the strong dependence of thermal conductivity of coal on temperature. Known empirical models for thermal conductivity include the models of Agroskin *et al*. (1970), Badzioch *et al*. (1964), Badzioch and Hawksley (1970) and Heidenreich *et al*. (1999). The latter two were chosen for this investigation. The thermophysical constants listed in Table 3.3 allow for the heat of reaction of devolatilization, which is assumed to stay constant throughout the whole process (Adesanya & Pham, 1995; Sadhukhan *et al*., 2011). In addition, thermophysical properties of the inert gas used during devolatilization can be estimated through empirical correlations or interpolation of thermophysical property measurements performed at different temperatures for the specific inert medium (Incropera *et al*., 2007). Values of density (ρ_g), gas viscosity (μ_g), gas thermal conductivity (k_g) and Prandtl number (Pr) are required for the calculation of the Reynolds number (Re) and the convective heat transfer coefficient (Equation (3.24)) of the inert gas flowing through the reactor system. For flow around spherical particles the Reynolds number is defined as (Incropera *et al*., 2007):

$$\mathrm{Re} = \frac{\rho_g v_g d_p}{\mu_g} \qquad \text{Equation (3.27)}$$

Table 3.3 Thermophysical constants used for the heat equation.

Thermophysical property	***Symbol***	***Value***	***Reference***
Stefan-Boltzmann constant	σ_b	5.67×10^{-8} W.m^{-2}.K^{-4}	(Incropera *et al*., 2007)
Emissivity of coal	$\varepsilon_{rad,s}$	0.95	(Omega Engineering Inc., 2012b)
Emissivity of reactor tube	$\varepsilon_{rad,t}$	0.30	(Omega Engineering Inc., 2012a)
Heat of reaction	ΔH_r	~300 kJ.kg^{-1}	(Adesanya & Pham, 1995)

3.4.2 Mass transfer considerations

An extensive mass transfer model with respect to the description of both the transport of gaseous products and tars has been proposed by Bliek *et al*. (1985). The use of this model,

however, requires knowledge regarding the specific properties and yields of the products formed. For the sake of simplicity Sadhukhan *et al*. (2011) proposed that the evolved gases and tars are envisaged as a single entity (*i.e.* volatile matter). The transport of water vapour (moisture) and volatiles through the porous matrix of coal/char can therefore be described by the conservation of mass equation. Pores of the coal/char structure, are assumed to be cylindrical in shape and connect the surface of the particle with the interior. Furthermore, the conservation of the solid reacting mass should also be taken into account and can therefore be written as:

$$\frac{\partial \rho_s}{\partial t} = -\left(R_v + R_a\right) \qquad \text{Equation (3.28a)}$$

Multiplication of both sides of Equation (3.28a) in order to account for the effect particle volume change yields the following:

$$v\frac{\partial \rho_s}{\partial t} = -v \cdot \left(R_v + R_a\right) \qquad \text{Equation (3.28b)}$$

Assuming the change in particle volume to be time dependent leads to the following expression:

$$\frac{\partial v\rho_s}{\partial t} = -v \cdot \left(R_v + R_a\right) \qquad \text{Equation (3.28c)}$$

Application of the chain rule, rearranging terms and division by the volume (v) yields the following equation as proposed by Sadhukhan *et al*., (2011) and Zhang *et al*. (2012):

$$v\frac{\partial \rho_s}{\partial t} + \rho_s \frac{\partial v}{\partial t} = -v \cdot \left(R_v + R_a\right) \qquad \text{Equation (3.28d)}$$

$$\frac{\partial \rho_s}{\partial t} = -\left(R_v + R_a\right) - \frac{\rho_s}{v}\frac{\partial v}{\partial t} \qquad \text{Equation (3.28e)}$$

The particle mass conservation (density) model not only includes for a change of density due to the creation of pores as a result of reaction but also due to a possible change in volume which dictates the behaviour of swelling and/or shrinking coals (Sadhukhan *et al*., 2011). For mass

transport of volatile species within the spherical porous solid the conservation of mass for species *i*, can however be expressed mathematically as:

$$\frac{\partial(\varepsilon\rho_i)}{\partial t}+\frac{1}{r^2}\frac{\partial\left(r^2\dot{n}_i\right)}{\partial r}=R_i \qquad \text{Equation (3.29)}$$

The total mass flux ($\acute{n}_i$) is considered to be a combination of the convective mass transport in the porous solid as well as the molecular diffusion of the gas species (Welty *et al*., 2008):

$$\dot{n}_i=\rho_i u-D_{eff}\frac{\partial}{\partial r}(\rho_i) \qquad \text{Equation (3.30)}$$

Therefore the conservation of mass for species *i* (moisture or volatiles), can be rewritten as:

$$\frac{\partial(\varepsilon\rho_i)}{\partial t}+\frac{1}{r^2}\frac{\partial}{\partial r}\left(r^2\rho_i u\right)-\frac{D'_{eff,i}}{r^2}\frac{\partial}{\partial r}\left(r^2\frac{\partial\rho_i}{\partial r}\right)=R_i \qquad \text{Equation (3.31)}$$

While the conservation (gas phase continuity) equation describing the overall transport of the gaseous mixture within the porous solid (moisture, volatiles as well as the presence of air initially in the porous solid) can be more specifically defined as (Bharadwaj *et al*., 2004; Peters, 2011; Sadhukhan *et al*., 2011):

$$\frac{\partial\left(\varepsilon\rho_{v,t}\right)}{\partial t}+\frac{1}{r^2}\frac{\partial}{\partial r}\left(r^2\rho_{v,t}u\right)=R_v+R_a \qquad \text{Equation (3.32)}$$

The importance of the molecular diffusion term has to be considered. The effect of the molecular diffusion of gaseous volatile species during the overall process has been considered to be negligible at high temperatures and -heat fluxes. This has been confirmed during investigations on the devolatilization of large wood particles by Bellais (2007) and Grønli (1996). During the drying stage of devolatilization molecular diffusion could not be neglected (Bellais, 2007; Grønli, 1996). For the sake of completeness however, effects of binary diffusion have been included for both moisture- and volatile evolution in this investigation. As for the heat equation, Sadhukhan *et al*. (2011) also adopted the inclusion of a term in the mass conservation law that could allow for any changes in particle volume during devolatilization. Inclusion of such

a term in the overall mass conservation equation can be accomplished by applying a similar mathematical strategy as was done for the heat equation, i.e:

$$v\frac{\partial(\varepsilon\rho_{v,t})}{\partial t}+\varepsilon\rho_{v,t}\frac{\partial(v)}{\partial t}+\frac{v}{r^2}\frac{\partial}{\partial r}\left(r^2\rho_{v,t}u\right)=v\cdot\left(R_v+R_a\right) \qquad \text{Equation (3.33a)}$$

$$\frac{\partial(\varepsilon\rho_{v,t})}{\partial t}+\frac{1}{r^2}\frac{\partial}{\partial r}\left(r^2\rho_{v,t}u\right)=R_v+R_a-\frac{\varepsilon\rho_{v,t}}{v}\frac{\partial v}{\partial t} \qquad \text{Equation (3.33b)}$$

The mass conservation equations for both volatile species and water vapour as a combination of the preceding developments can therefore be written as (Bharadwaj *et al.*, 2004):

$$\frac{\partial(\varepsilon\rho_v)}{\partial t}+\frac{1}{r^2}\frac{\partial}{\partial r}\left(r^2\rho_v u\right)-\frac{D'_{eff,v}}{r^2}\frac{\partial}{\partial r}\left(r^2\frac{\partial\rho_v}{\partial r}\right)=R_v-\frac{\varepsilon\rho_v}{v}\frac{\partial v}{\partial t} \qquad \text{Equation (3.34a)}$$

$$\frac{\partial(\varepsilon\rho_a)}{\partial t}+\frac{1}{r^2}\frac{\partial}{\partial r}\left(r^2\rho_a u\right)-\frac{D'_{eff,a}}{r^2}\frac{\partial}{\partial r}\left(r^2\frac{\partial\rho_a}{\partial r}\right)=R_a-\frac{\varepsilon\rho_a}{v}\frac{\partial v}{\partial t} \qquad \text{Equation (3.34b)}$$

Effective diffusion coefficients are considered to take the Knudsen effect into account. The above equations are formulated with the following boundary- and initial conditions (Bharadwaj *et al.*, 2004; Peters, 2011; Sadhukhan *et al.*, 2011):

At $t=0$ for $0\le r\le R_p$; $\quad p=p_0$ or $\rho_{v,t}=\rho_{air,T_0}$ and $\rho_i=0;\quad i=a,v$ Equation (3.35a)

For $t>0$ at $r=0;\quad \frac{\partial\rho_{v,t}}{\partial r}=\frac{\partial\rho_i}{\partial r}=0;\quad i=a,v$ Equation (3.35b)

For $t>0$ at $r=R_p;\quad \rho_{v,t}=\rho_{air,T_f}$ and $\rho_i=0;\quad i=a,v$ Equation (3.35c)

The velocity term (u) of the convective transport of total moisture and volatiles in the radial particle direction can be obtained using Darcy's law for porous solids (Bellais, 2007; Grønli, 1996; Sadhukhan *et al.*, 2011):

$$u=-\frac{K_p}{\mu_m}\cdot\frac{\partial p_{v,t}}{\partial r} \qquad \text{Equation (3.36)}$$

The total pressure- and partial pressure dependence of the gaseous mixture and volatile species can be assumed to follow the ideal gas law (Sadhukhan *et al*., 2011):

$$p_{v,t} = \frac{\rho_{v,t} R T_s}{M_{gv}} \qquad \text{Equation (3.37a)}$$

$$p_i = \frac{\rho_i R T_s}{M_i}; \quad i = a, v \qquad \text{Equation (3.37b)}$$

Empirical correlations and/or models are also employed for estimating the characteristic properties dictating the conservation of mass. Values of mass transfer constants and empirical equations are listed in Tables 3.4 and 3.5 respectively.

Table 3.4 Characteristic constants used for the mass transfer equation.

Characteristic property	***Symbol***	***Value***	***Reference***
Permeability of coal	K_p	1×10^{-11} m^2	(Borghi *et al*., 1985)
Molecular weight of devolatilization gas	M_{gv}	20 g.mol^{-1}	(Gavalas & Oka, 1978)
Molecular weight of devolatilization tars	M_t	325 g.mol^{-1} or taken from SEC results	(Gavalas & Oka, 1978)
Lennard-Jones constant for tar	$\frac{\varepsilon_{L,t}}{\kappa}$	660	(Reid *et al*., 1967; Reidelbach, 1979)
Lennard-Jones constant for gas	$\frac{\varepsilon_{L,gv}}{\kappa}$	136	(Reid *et al*., 1967; Reidelbach, 1979)
Lennard-Jones constant for air	$\frac{\varepsilon_{L,air}}{\kappa}$	97	(Welty *et al*., 2008)
Lennard-Jones constant for tar (Collision diameter)	σ_t	10 Å	(Reid *et al*., 1967; Reidelbach, 1979)
Lennard-Jones constant for gas (Collision diameter)	σ_{gv}	3.4 Å	(Reid *et al*., 1967; Reidelbach, 1979)
Lennard-Jones constant for air (Collision diameter)	σ_{air}	3.62 Å	(Welty *et al*., 2008)

From these tables the permeability of the coal is assumed to stay constant throughout the description of the process. This is, however, not true but from the work of Sadhukhan *et al.* (2011), the value used has been found to provide a more than adequate description of the devolatilization process of large coal particles. An average molecular mass of coal volatiles can be estimated with application of the empirical model provided in Table 3.5.

Table 3.5 Auxiliary equations used in the conservation of mass.

Characteristic property	***Empirical correlation/equation***	***Equation no.:***
Coal porosity	$\varepsilon \approx \frac{\rho_{s,k} - \rho_s}{\rho_{s,k}}$ Unit: [-]	Equation (3.38)
Viscosity of volatiles (Reid *et al.*, 1967)	$\mu_v = \frac{2\times10^{-26} \cdot (M_v T_s)^{0.5}}{\sigma_v^2 \Omega_v}$ Unit: [Pa.s]	Equation (3.39)
Lennard-Jones constants for tar-gas mixture (Reid *et al.*, 1967)	$\frac{\varepsilon_{L,gt}}{\kappa} = \left(\frac{\varepsilon_{L,t}}{\kappa} \cdot \frac{\varepsilon_{L,gv}}{\kappa} \right)^{0.5}$ and $\sigma_{gt} = 0.5 \cdot (\sigma_{gv} + \sigma_t)$ Unit: [-]	Equation (3.40)
Lennard-Jones constants for volatile-air mixture (Reid *et al.*, 1967)	$\frac{\varepsilon_{L,v-air}}{\kappa} = \left(\frac{\varepsilon_{L,gt}}{\kappa} \cdot \frac{\varepsilon_{L,air}}{\kappa} \right)^{0.5}$ and $\sigma_{vair} = 0.5 \cdot (\sigma_{gt} + \sigma_{air})$ Unit: [-]	Equation (3.41)
Lennard-Jones equations for viscosity determinations (Reid *et al.*, 1967; Reidelbach, 1979)	$\Omega_{v,i} = 1.165 \left(\frac{\kappa T_s}{\varepsilon_{L,i}} \right)^{-0.149} + 0.525 \exp\left(-0.773 \frac{\kappa T_s}{\varepsilon_{L,i}} \right)$ $\Omega_v = 0.5 \cdot (\Omega_{v,t} + \Omega_{v,g})$ Unit: [-]	Equation (3.42) Equation (3.43)
Lennard-Jones equations for mass transfer determinations (Perry & Green, 1997)	$\Omega_{D,i,j} = \left\{ 44.54 \left(\frac{\kappa T_s}{\varepsilon_{L,i,j}} \right)^{-4.909} + 1.911 \left(-0.773 \frac{\kappa T_s}{\varepsilon_{L,i,j}} \right)^{-1.575} \right\}$ $\Omega_{D,ij} = 0.5 \cdot (\Omega_{D,i} + \Omega_{D,j})$ Unit: [-]	Equation (3.44) Equation (3.45)

Table 3.5 Auxiliary equations used in the conservation of mass (cont'd).

Characteristic property	*Empirical correlation/equation*	*Equation no.:*
Viscosity of water vapour (Bellais, 2007)	$\mu_a = -1.47\times10^{-6} + 3.78\times10^{-8}\cdot T_s$ Unit: [Pa.s]	Equation (3.46)
Molecular weight of total volatiles (Seader & Henley, 2006)	$M_v = \frac{2}{(1/M_t)+(1/M_{gv})}$ Unit: [g.mol^{-1}]	Equation (3.47)
Binary diffusion coefficient for water vapour in air (Grønli, 1996)	$D_{a-air} = 1.192\times10^{-4}\cdot\left(\frac{T_s^{1.75}}{p}\right)$ Unit: [m^2 s^{-1}]	Equation (3.48)
Binary diffusion coefficient for tar in gas (Welty *et al.*, 2008)	$D_{t-gv} = 1.86\times10^{-7}\cdot\left(\frac{T_s^{1.5}}{p\sigma_{gt}^2\Omega_{D,gt}}\right)\cdot\left\{\frac{1}{M_t}+\frac{1}{M_{gv}}\right\}^{0.5}$ Unit: [m^2 s^{-1}]	Equation (3.49)
Binary diffusion coefficient for volatiles in air (Welty *et al.*, 2008)	$D_{v-air} = 1.86\times10^{-7}\cdot\left(\frac{T_s^{1.5}}{p\sigma_{vair}^2\Omega_{D,vair}}\right)\cdot\left\{\frac{1}{M_v}+\frac{1}{M_{air}}\right\}^{0.5}$ Unit: [m^2 s^{-1}]	Equation (3.50)
Knudsen diffusion of species, *i* (Welty *et al.*, 2008)	$D_{iK} = 4850\tilde{d}_{pore}\cdot\sqrt{\frac{T_s}{M_i}};\quad i=a,v$ Unit: [m^2 s^{-1}]	Equation (3.51)
Effective diffusion coefficient of species, *i.* (Welty *et al.*, 2008)	$D'_{eff,i} = \frac{1}{D_{i-air}}+\frac{1}{D_{i,K}};\quad i=a,v$ Unit: [m^2 s^{-1}]	Equation (3.51)
Effective diffusion coefficient of species *i*, in random pores (Welty *et al.*, 2008)	$D_{eff,i} = \frac{\varepsilon}{\tau}\cdot D'_{eff,i}$ Unit: [m^2 s^{-1}]	Equation (3.52)

The values of porosity change can either be estimated via Equation (3.38) or be determined experimentally (Sadhukhan *et al*., 2011). In addition, to account for the effect of volume change on the thermal- and mass transfer properties, volume change as defined by the swelling/shrinkage ratio can be determined qualitatively from non-isothermal or isothermal measurements (Sadhukhan *et al*., 2011). Other investigations involving volume changes of coals have also shown that thermo-mechanical analysis (TMA) is a valuable tool for determining the thermal expansion of coals with temperature (Gupta, 2007). An empirical model for thermal expansion/shrinkage can therefore be used to describe the swelling/shrinkage term in both the heat- and mass equation.

3.5 Evaluation and validation procedure of the combined model

The description of the complete devolatilization process involves the combination and the subsequent evaluation of the preceding equations in order to determine specified parameters as a function of both time and particle radius. The set of descriptive partial differential equations (PDE's) and auxiliary equations can be solved numerically according to a finite element method with the aid of COMSOL Multiphysics® 4.3 simulation software. From a coal conversion perspective this simulation software has been successfully used in the simulation of CO_2 sequestration studies (Liu & Smirnov, 2007), underground gasification (Sarraf *et al*., 2011) and fires in bulk materials and coal dumps (Krause *et al*., 2005).

Kinetic measurements on smaller coal particles enable the decoupling of kinetics from the overall process and the estimation of kinetic parameters in a strictly kinetic-controlled environment. The obtained kinetic parameters are provided as input to the COMSOL Multiphysics® 4.3 simulation software and therefore not solved by parameter regression as seen in most investigations. The numerical reproduction of the modelled conversion curves are evaluated against the experimental data via a visual collocation method. In addition, *QOF* is assessed for all experiments with the aid of Equation (3.16).

Bibliography

Abhari, R., & Isaacs, L.L. 1990. Drying kinetics of lignite, subbituminous coals and high-volatile bituminous coals. *Energy & Fuels*, 4: 448-452.

Aboulkas, A., El Harfi, K., Nadifiyine, M. & Benchanaa, M. 2011. Pyrolysis behaviour and kinetics of Moroccan oil shale with polystyrene. *Journal of Petroleum and Gas Engineering,* 2(6): 108-117.

Aboyade, A.O., Hugo, T.J., Carrier, M., Meyer, E.L., Stahl, R., Knoetze, J.H. & Görgens, J.F. 2011. Non-isothermal kinetic analysis of the devolatilization of corn cobs and sugar cane bagasse in an inert atmosphere. *Thermochimica Acta,* 517: 81-89.

Aboyade, A.O., Carrier, M., Meyer, E.L., Knoetze, J.H. & Görgens, J.F. 2012. Model fitting kinetic analysis and characterisation of the devolatilization of coal blends with corn and sugarcane residues. *Thermochimica Acta,* 530: 95-106.

Adesanya, B. A. & Pham, H.N. 1995. Mathematical modelling of devolatilization of a large coal particle in a convective environment. *Fuel* , 74(6): 896–902.

Agarwal, P.K., Genetti, W.E. & Lee, Y.Y. 1984a. Model for devolatilization of coal particles in fluidized beds. *Fuel,* 63(8): 1157-1165.

Agarwal, P.K., Genetti, W.E. & Lee, Y.Y. 1984b. Devolatilization of large coal particles in fluidized beds. *Fuel,* 63(12): 1748-1752.

Agarwal, P.K. 1985. Distributed kinetic parameters for methane evolution during coal pyrolysis. *Fuel,* 64(6): 870-872.

Agarwal, P.K., Agnew, J.B., Ravindran, N. & Weimann, R. 1987. Distributed kinetic parameters for the evolution of gaseous species in the pyrolysis of coal. *Fuel*, 66(8): 1097-1106.

Agroskin, A.A., Gonczarow, E.I., Makeev, L.A. & Jakunin, W.P. 1970. Thermal capacity and heat of pyrolysis of Donbass coal. *Koki Chimija*, 5:8-13.

Alonso, M.J.G., Boreggo, A.G., Alvarez, D. & Menéndez, R. 1999. Pyrolysis behaviour of pulverised coals at different temperatures. *Fuel,* 78: 1501-1513.

Alonso, M.J.G., Alvarez, D., Borrego, A.G., Menéndez, R. & Marbán, G. 2001. Systematic effects of coal rank and type on the kinetics of coal pyrolysis. *Energy & Fuels,* 15(2): 413-428.

Antal, M.J. & Várhegyi, G. 1995. Cellulose pyrolysis kinetics: The current state of knowledge. *Industrial and Engineering Chemistry Research*, 34: 703-717.

Anthony, D.B., Howard, J.B., Hottel, H.C. & Meissner, H.P. 1975. Rapid devolatilization of pulverised coal. *Symposium (International) on Combustion*, 15(1): 1303-1317.

Anthony, D.B., Howard, J.B., Hottel, H.C. & Meissner, H.P. 1976. Rapid devolatilization and hydrogasification of bituminous coal. *Fuel*, 55:121-128.

Arenillas, A., Rubiera, F., Pevida, C. & Pis, J.J. 2001. A comparison of different methods of predicting coal devolatilization kinetics. *Journal of Analytical and Applied Pyrolysis,* 58-59: 685-701.

Badzioch, S., Gregory, D.R. & Field, M.A. 1964. Investigation of the temperature variation of the thermal conductivity and thermal diffusivity of coal. *Fuel,* 43: 267.

Badzioch, S. & Hawksley, P.G.W. 1970. Kinetics of thermal decomposition of pulverised coal particles. *Ind. Eng. Chem. Process Des. Dev., 9: 521-527.*

Bellais, M. 2007. Modelling of the pyrolysis of large wood particles. Stockholm: The Royal Institute of Technology (KTH). Sweden. (Thesis-Ph.D). 105p.

Bharadwaj, A., Baxter, L.L. & Robinson, A.L. 2004. Effects of intraparticle heat and mass transfer on biomass devolatilization: experimental results and model predictions. *Energy & Fuels,* 18: 1021-1031.

Bliek, A., Van Poelje, W.M., Van Swaaij, W.P.M. & Van Beckhum, F.P.H. 1985. Effects of intraparticle heat and mass transfer during devolatilization of a single coal particle. *Journal of the American Institute of Chemical Engineers,* 31(10): 1666-1681.

Boiko, E. A. 2000. Research on kinetics of the thermal processing of brown coals of various oxidative aging degree using the non-isothermal method. *Thermochimica Acta*, 348: 97-104.

Borghi, G., Sarofim, A.F. & Beer, J.M. 1985. A model of coal devolatilization and combustion in fluidized beds. *Combustion & Flame,* 61: 1–16.

Braun, R.L. & Burnham, A.K. 1987. Analysis of chemical reaction kinetics using a distribution of activation energies and simpler models. *Energy & Fuels,* 1(2): 153-161.

Bunt, J.R. & Waanders, F.B. 2008. Identification of the reaction zones occurring in a commercial-scale Sasol-Lurgi FBDB gasifier. *Fuel*, 87(10-11): 1814-1823.

Burnham, A.K. & Braun, R.L. 1999. Global kinetic analysis of complex materials. *Energy & Fuels,* 13(1): 1-22.

Burnham, A.K., Schmidt, B.J. & Braun, R.L. 1995. A test of the parallel reaction model using kinetic measurements on hydrous pyrolysis residues. *Organic Geochemistry,* 23(10): 931-939.

Caballero, J.A. & Conesa, J.A. 2005. Mathematical considerations for non-isothermal kinetics in thermal decomposition. *Journal of Analytical and Applied Pyrolysis,* 73: 85-100.

Cai, J. & Liu, R. 2008. New distributed activation energy model: numerical solution and application to pyrolysis kinetics of some types of biomass. *Bioresource Technology*, 99: 2795-2799.

Coats, A.W. & Redfern, J.P. 1964. Kinetic parameters from thermogravimetric data. *Nature (London),* 201: 68-69.

Conesa, J.A., Marcilla, A., Caballero, J.A. & Font, R. 2001. Comments on the validity and utility of the different methods for kinetic analysis of thermogravimetric data. *Journal of Analytical and Applied Pyrolysis,* 58-59: 617-633.

Constable, F.H. 1925. The mechanism of catalytic decomposition. *Proceedings of the Royal Society of London Series A,* 108: 355-385.

Donskoi, E. & McElwain, D.L.S. 1999. Approximate modelling of coal pyrolysis. *Fuel,* 78: 825-835.

Donskoi, E. & McElwain, D.L.S. 2000. Optimization of coal pyrolysis modelling. *Combustion and Flame*, 122: 359-367.

Friedman, H.L. 1964. Kinetics of thermal degradation of char-forming plastics from thermogravimetry. Application to a phenolic plastic. *Journal of Polymer Science, Part C: Polymer Symposia,* 6(1): 183-195.

Gavalas, G.R. & Oka, M. 1978. Characterisation of the heavy products of coal pyrolysis. *Fuel,* 57(5): 285-288

Grønli, M.G. 1996. A theoretical and experimental study of the thermal degradation of biomass. Trondheim: The Norwegian University of Science and Technology. Norway. (Thesis-Ph.D). 339p.

Grønli, M.G., Várhegyi, G. & Di Blasi, C. 2002. Thermogravimetric analysis and devolatilization kinetics of wood. *Industrial and Engineering Chemistry Research,* 41: 4201-4208.

Gupta, R. 2007. Advanced Coal Characterisation: A Review. *Energy & Fuels*, 21: 451-460.

Gürüz, G.A., Üçtepe, Ü. & Durusoy, T. 2004. Mathematical modelling of thermal decomposition of coal. *Journal of Analytical and Applied Pyrolysis,* 71: 537-551.

Heidenreich, C.A., Yan, H.M. & Zhang, D.K. 1999. Mathematical modelling of pyrolysis of large coal particles – estimation of kinetic parameters for methane evolution. *Fuel,* 78: 557-566.

Howard, J.B., Anthony, D.B., Hottel, H.C. & Meissner, H.P. 1976. Rapid devolatilization and hydrogasification of bituminous coal. *Fuel*, 55: 121-128.

Incropera, F.P., Dewitt, D.P., Bergman, T.L. & Lavine, A.S. 2007. Fundamentals of heat and mass transfer. United States of America: John Wiley & Sons, Inc. 997p.

Kristiansen, A. 1996. Understanding coal gasification. London : IEA Coal Research. 70 p.

Koch, E., Juntgen, H. & Peters, W. 1969. Non-isothermal reaction kinetics of coal pyrolysis (in German). *Brennstoffchemie,* 50: 366-373.

Kök, M.V., Özbas, E., Karacan, O. & Hicyilmaz, C. 1998. Effect of particle size on coal pyrolysis. *Journal of Analytical and Applied Pyrolysis*, 45: 103-110.

Krause, U., Schmidt, M. & Lohrer, C. 2005. Computations on the coupled heat and mass transfer during fires in bulk materials, coal deposits and waste dumps. Paper presented at the annual COMSOL Multiphysics User's conference, Frankfurt, Germany. http://www.comsol.com/papers/1177.pdf Date of access: 25 Mar. 2012.

Kumar, P. & Kunzru, D. 1985. Modelling of naphtha pyrolysis. *Industrial & Engineering Chemistry Process Design and Development,* 24: 774-782.

Kunii, D. & Levenspiel, O. 1969. Fluidization engineering. New York: John Wiley & Sons Publishing. p. 210.

Lázaro, M.-J., Moliner, R. & Suelves, I. 1998. Non-isothermal versus isothermal technique to evaluate kinetic parameters of coal pyrolysis. *Journal of Analytical and Applied Pyrolysis,* 47: 111-125.

Li, X., Song, H., Wang, Q., Meesri, C., Wall, T. & Yu, J. 2009. Experimental study on drying and moisture re-adsorption kinetics of an Indonesian low rank coal. *Journal of Environmental Sciences Supplement*, S127-S130.

Liu, G. & Smirnov, A.F. 2007. Numerical modelling of CO_2 sequestration in coal-beds with variable saturation on COMSOL. Paper presented at the annual international COMSOL Multiphysics User's conference, Boston, New York.
http://www.comsol.com/papers/3027/download/Liu_Guoxiang.pdf Date of access: 25 Mar. 2012.

Lu, G.Q. & Do, D.D. 1991. A kinetic model for coal reject pyrolysis at low heating rates. *Fuel Processing Technology,* 28: 35-48.

Mani, T., Murugan, P. & Mahinpey, N. 2009. Determination of distributed activation energy model kinetic parameters using simulated annealing optimization method for non-isothermal pyrolysis of lignin. *Industrial & Engineering Chemistry Research,* 48: 1464-1467.

Mianowski, A. & Radko, T. 1993. Isokinetic effect in coal pyrolysis. *Fuel,* 72(11): 1537-1539.

Misra, M.K. & Essenhigh, R.H. 1988. Release of volatiles from pyrolysing coal particles: Relative roles of kinetics, heat transfer and diffusion. *Energy & Fuels,* 2(4): 371-385.

Miura, K. 1995. A new and simple method to estimate f(E) and k0(E) in the distributed activation energy model from three sets of experimental data. *Energy & Fuels,* 9(2): 302-307.

Narayan, R. & Antal, M.J. 1996. Thermal lag, fusion and the compensation effect during biomass pyrolysis. *Industrial & Engineering Chemistry Research,* 35: 1711-1721.

Niksa, S. & Kerstein, A.R. 1991. FLASHCHAIN theory for rapid coal devolatilization kinetics. 1. Formulation. *Energy & Fuels,* 5: 647-665.

Olivella, M.Á. & De Las Heras, F.X.C. 2006. Non-isothermal thermogravimetry of Spanish fossil fuels. *Oil Shale,* 23(4): 340-355.

Olivella, M.Á. & De Las Heras, F.X.C. 2008. Evaluation of linear kinetic methods from pyrolysis data of Spanish oil shales and coals. *Oil Shale,* 25(2): 227-245.

Omega Engineering, INC. 2012a. Emissivity of common materials: metals index. http://www.omega.com/literature/transactions/volume1/emissivitya.html Date of access: 10 Apr. 2012.

Omega Engineering, INC. 2012b. Emissivity of common materials: non-metals index. http://www.omega.com/literature/transactions/volume1/emissivityb.html Date of access: 10 Apr. 2012.

Perry, R.H. & Green, D.W. 1997. Perry's chemical engineers' handbook. 7th ed.. New York: McGraw-Hill. p. 5-48 – 5-54.

Peters, B. 2011. Validation of a numerical approach to model pyrolysis of biomass and assessment of kinetic data. *Fuel,* 90: 2301-2314.

Reid, R.C.J., Prausnitz, J.M. & Sherwood, T.K. 1967. The properties of liquids and gases. 2nd ed. New York: McGraw-Hill.

Reidelbach, H. & Summerfield, R. 1975. Kinetic model for coal pyrolysis optimization. *169th Nat. Meet. Am. Chem. Soc., Div., Fuel Chem. Preprint ,* 20(l): 161.

Sadhukhan, A.K., Gupta, P. & Saha, R.K. 2011. Modelling and experimental investigations on the pyrolysis of large coal particles. *Energy & Fuels*, 25: 5573-5583.

Sarraf, A., Mmbaga, J.P., Gupta & Hayes, R.E. 2011. Modelling cavity growth during underground coal gasification. Paper presented at the annual international COMSOL Multiphysics User's conference, Boston, New York. http://www.comsol.com/papers/10753/ download/shirazi_paper.pdf Date of access: 25 Mar. 2012.

Seader, J.D. & Henley, E.J. 2006. Separation process principles. 2nd ed. New Jersey: John Wiley & Sons, Inc. 755p.

Serio, M. A., Hamblen, D. G., Markham, J. R. & Solomon, P. R. 1987. Kinetics of volatile product evolution in coal pyrolysis: Experiment and theory. *Energy & Fuels*, 1(2): 138-152.

Shih, S.M. & Sohn, H.Y. 1980. Non-isothermal determination of the intrinsic kinetics of oil generation from oil shale. *Industrial & Engineering Chemistry Design and Development,* 19: 426-431.

Smoot, L.D. & Pratt, D.T. 1979. Pulverised coal combustion and gasification. New York : Plenum Press.

Smoot, L.D. 1981. Pulverised coal diffusion flames: A perspective through modelling. *Eighteenth Symposium (International) on Combustion, The Combustion Institute,* 18(1): 1185-1202.

Solomon, P. R., Serio, M. A. & Suuberg, E. M. 1992. Coal pyrolysis experiments: Kinetic rates and mechanisms. *Progress in Energy and Combustion Science*, 18: 133-220.

Solomon, P.R., Fletcher, T.H. & Pugmire, R.J. 1993. Progress in coal pyrolysis. *Fuel*, 72:587-597.

Strezov, V., Lucas, J.A. & Strezov, L. 2004. Experimental and modelling of the thermal regions of activity during pyrolysis of bituminous coals. *Journal of Analytical and Applied Pyrolysis*, 71:375-392.

Stubington, J.F. & Sumaryono. 1984. Release of volatiles from large coal particles in a hot fluidized bed. *Fuel,* 63(7): 1013-1019.

Thakur, D.S. & Nuttal, H.E. 1987. Kinetics of pyrolysis of Moroccan oil shale by thermogravimetry. *Industrial & Engineering Chemistry Research,* 26: 1351-1356.

Tomeczek, J. & Kowol, J. 1990. Temperature field within a devolatilizing coal particle. *Canadian Journal of Chemical Engineering,* 69: 286-293.

Trimm, D.L. & Turner, C.J. 1981. The pyrolysis of propane. I. Production of gases, liquids and carbon. *Journal of Chemical Technology & Biotechnology,* 31: 195-204.

Tsang, T.H.T. 1980. Modelling heat and mass transfer during coal block gasification. Austin: University of Texas. USA. (Thesis-Ph.D). 390p.

Van Heek, K. H. & Hodek, W. 1994. Structure and pyrolysis behaviour of different coals and relevant model substances. *Fuel*, 73(6): 886-896.

Welty, J.R., Wicks, C.E., Wilson, R.E. & Rorrer, G.L. 2008. Fundamentals of momentum, heat and mass transfer. 5th ed. New Jersey: John Wiley & Sons, Inc. 711p.

Wildegger-Gaissmaier, A.E. & Agarwal, P.K. 1990. Drying and devolatilization of large coal particles under combustion conditions. *Fuel,* 69: 44-52.

Yang, H., Chen, H., Ju, F., Yan, R. & Zhang, S. 2007. Influence of pressure on coal pyrolysis and char gasification. *Energy & Fuels*, 21: 3165-3170.

Yip, K., Wu, H. & Zhang, D-.K. 2009. Mathematical modelling of Collie coal pyrolysis considering the effect of steam produced in situ from coal inherent moisture and pyrolytic water. *Proceedings of the Combustion Institute,* 32: 2675-2683.

Yongjiang, X., Huaqing, X., Hongyan, W., Zhiping, L. & Chaohe, F. 2011. Kinetics of isothermal and non-isothermal pyrolysis of oil shale. *Oil Shale,* 28(3): 415-424.

Yue, C. 1995. Experimental and modelling study of pitch pyrolysis kinetics. Vancouver: University of British Columbia. CAN. (Thesis-Ph.D). 242p.

Zhang, K., You, C. & Li, Y. 2012. Experimental and numerical investigation on the pyrolysis of single course lignite particles. *Korean Journal of Chemical Engineering,* 29(4): 540-548.